Top Curr Chem (2016) 370: 1–28
DOI: 10.1007/978-3-319-22942-3_1

Luminescent Silica Nanoparticles Featuring Collective Processes for Optical Imaging

Enrico Rampazzo, Luca Prodi, Luca Petrizza, and Nelsi Zaccheroni

Abstract The field of nanoparticles has successfully merged with imaging to optimize contrast agents for many detection techniques. This combination has yielded highly positive results, especially in optical and magnetic imaging, leading to diagnostic methods that are now close to clinical use. Biological sciences have been taking advantage of luminescent labels for many years and the development of luminescent nanoprobes has helped definitively in making the crucial step forward in in vivo applications. To this end, suitable probes should present excitation and emission within the NIR region where tissues have minimal absorbance. Among several nanomaterials engineered with this aim, including noble metal, lanthanide, and carbon nanoparticles and quantum dots, we have focused our attention here on luminescent silica nanoparticles. Many interesting results have already been obtained with nanoparticles containing only one kind of photophysically active moiety. However, the presence of different emitting species in a single nanoparticle can lead to diverse properties including cooperative behaviours. We present here the state of the art in the field of silica luminescent nanoparticles exploiting collective processes to obtain ultra-bright units suitable as contrast agents in optical imaging and optical sensing and for other high sensitivity applications.

Keywords Luminescent contrast agents nanomedicine • Luminescent probes • Optical imaging • Silica nanoparticles

Contents

E. Rampazzo, L. Prodi (✉), L. Petrizza, and N. Zaccheroni
Dipartimento di Chimica, G. Ciamician, Via Selmi 2, 40126 Bologna, Italy
e-mail: luca.prodi@unibo.it

Abbreviations

Φ	Quantum yield
AFM	Atomic force microscopy
AOT	Bis(2-ethylhexyl)sulfosuccinate sodium salt
APTES	3-Aminopropyltriethoxysilane
BHQ	Black hole quenchers
CT	Computed tomography
CTAB	Hexadecyltrimethylammonium bromide
Cy5	Cyanine 5
Cy5.5	Cyanine 5
Cy7	Cyanine 7
DDSNP	Dye doped silica nanoparticle
DLS	Dynamic light scattering
EPR	Enhanced permeability and retention effect
ET	Energy transfer
FAM	Fluorescein amidite
FRET	Förster resonance energy transfer
IR780	I2-[2-[2-Chloro-3-[(1,3-dihydro-3,3-dimethyl-1-propyl-2*H*-indol-2-ylidene)ethylidene]-1-cyclohexen-1-yl]ethenyl]-3,3-dimethyl-1-propylindolium (Cy7 dye)
MRI	Magnetic resonance imaging
NIR	Near infrared region
nm	Nanometre
NP	Fluorescent silica nanoparticles
ORMOSIL	Organic modified silica
PDT	Photodynamic therapy
PEG	Polyethyleneglycol, ethylene oxide, ethylene glycol
Plus NP	NP Pluronic silica nanoparticle
PPO	Poly(propylene oxide)
PS	Phosphatidylserine
PTT	Photothermal therapy
QD	Quantum dot
R6G	Rhodamine 6G
ROX	Rhodamine-X, rhodamine 101
$Ru(bpy)_3^{2+}$	Tris(2,2′-bipyridine)ruthenium(II)

TEM	Transmission electron microscopy
TEOS	Tetraethylorthosilicate
TGA	Thermo gravimetric analysis
VTES	Triethoxyvinylsilane

1 Introduction

Despite the great multidisciplinary research effort worldwide and the great steps forward in the understanding and treatment of cancer and other diseases such as diabetes and Alzheimer's, there is still much to be solved. Besides improved and personalized therapies, early diagnosis is fundamental to reduce morbidity and consequently mortality. With this aim, many different imaging techniques [1] are used to spot these diseases and monitor anatomical and functional changes [2–7]. The various imaging modalities already in clinical use differ significantly in basic features such as resolution, time of analysis, penetration depth, and costs, but, in general, they still suffer from low sensitivity and low contrast. The development of other imaging methods to speed their clinical translation becomes essential in this scenario, an aim that can be obtained by optimizing exogenous contrast agents. These imaging tools need to be stable in physiological conditions to enable selective targeting, high signal-to-noise ratio, and optimized time of circulation and clearance [8, 9].

Optical imaging is one of the most promising diagnostic techniques and it is already close to clinical application being habitually applied in preclinical studies on small animals [10, 11]. It presents the great advantages of high sensitivity, short time of analysis, and low cost, with a few drawbacks linked to small penetration depth (1–20 mm) and to relatively limited resolution. Because of the scattering of blood, tissues, and other biological components, deeper penetration in in vivo imaging can be obtained only by working in the NIR range, in the so-called biological optical transparency window (650–1800 nm) [12]. The use of NIR light absorption and emission ensures a low auto-fluorescence and tissue damage—a possible concern when long-term UV excitation is required—and reduced light scattering. It should be mentioned, however, that two water absorption peaks (centred around 980 and 1450 nm) also fall in this spectral range, and therefore the possible non-negligible and harmful local heating of biological samples when exciting via laser light in this window [13] has to be carefully evaluated. On the other hand, optical imaging presents exceptional versatility: (1) the luminescence process can start with excitation different from photo-excitation, obtaining luminescence in dark conditions as in the case of chemiluminescence [14], electro-chemiluminescence [15, 16], and thermochemiluminescence [17]; (2) light can be exploited not only for diagnostic purposes but also for therapeutic treatments (for example in the photodynamic and photothermal therapies, PDT and PTT respectively) [18, 19].

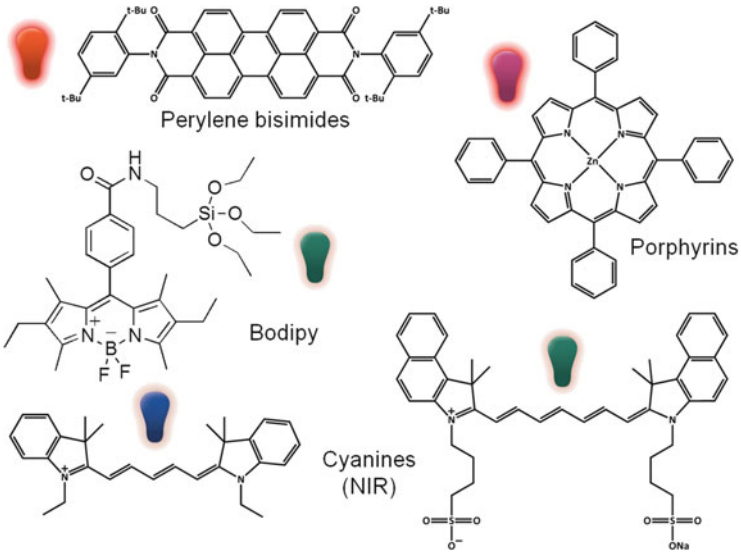

Fig. 1 Some families of organic luminophores presenting NIR absorption and/or emission

The most studied and common contrast agents for this kind of imaging are fluorescent molecules, in particular for in vivo applications as NIR absorbing and emitting luminophores [20]. There are some deeply investigated families of organic dyes with suitable features such as cyanines, phthalocyanines, and bodipys, to name a few (Fig. 1), but they also exhibit very poor water solubility and, generally, decreasing quantum yield, moving the emission towards the red part of the spectrum. Many different derivatizations of these molecules have been proposed to overcome these limitations and also to introduce targeting functions, usually at the expense of demanding synthetic procedures. Moreover, low weight (molecular) contrast agents suffer from fast clearance which decreases their ability to reach all organs because of the short available time of measurement for image acquisition.

In this context, the use of nanostructured contrast agents can provide interesting solutions [21, 22]. Lots of nanomaterials have been proposed which include dye doped nanoparticles [23] (for example, luminescent silica nanoparticles [8, 24]) or intrinsically luminescent materials (for example, quantum dots) [25, 26]. The use of non-toxic materials such as silica have inherent advantages, although dimension - and surface - related hazards need to be investigated for each system. The silica matrix can also be seen as a robust container able to ensure an almost constant chemical environment, and to improve chemical stability and resistance to photobleaching of the doping dyes. It is also transparent to visible light and therefore inert towards photophysical processes that involve the photoactive species embedded in the matrix [24, 27].

It has to be emphasized, however, that on passing from molecules to nanoparticles the molecular weight is increased by few orders of magnitude and

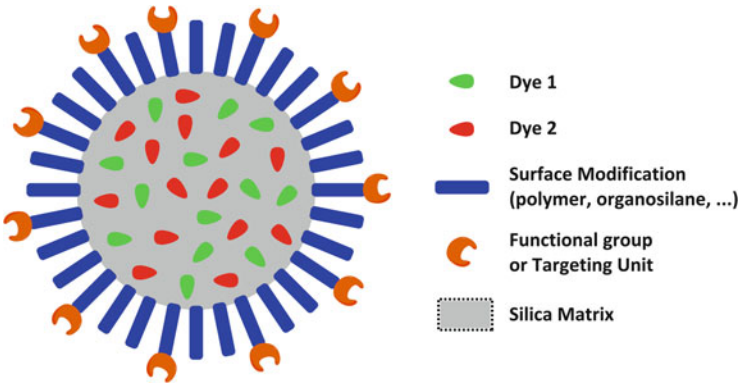

Fig. 2 Schematization of a dye doped silica nanoparticle with a surface derivatization and presenting targeting functions

this could cause possible viscosity problems with the solution being injected for in vivo applications in the case of low sensitivity techniques such as MRI and CT [28]. This is not the case with optical imaging where highly luminescent materials lead to very high sensitivity, and low concentrations of contrast agents are required. In the case of luminescent silica nanoparticles, each nanoparticle contains many dyes and this can lead to an increase in the overall signal-to-noise ratio. This goal can be reached thanks to the great versatility of these nanotemplates, which is largely because of the many different, typically mild, and non-cost effective synthetic strategies which allow the efficient derivatization of the inner core, the outer surface, or the mixing of different materials and the production of core-shell and multi-shell architectures [29]. All this opens up possibilities for the preparation of customized species for a large variety of applications (Fig. 2).

Bearing in mind the preparation of contrast agents for optical imaging in vivo, the ability to introduce antibodies, peptides, or proteins to guide localization in the target area is of fundamental interest, even if the biochemical difference existing among healthy and unhealthy tissues gives rise to the well-known *enhanced permeability and retention* effect (EPR). EPR consists in the preferential accumulation in the malignant areas of nanoobjects exceeding around 5 nm in diameter, an effect, however, which is not very linear, homogeneous, or predictable, and which can be considered really effective only in areas where the lesion is quite big and vascularised; it is not, therefore, reliable for the specific detection of early stage (sub-millimetre) metastasis. The few nano-preparations exploiting the EPR effect are already approved for clinical use and they consist of some nano-therapeutics mostly based on liposomal systems. However, for early diagnosis a targeted approach is necessary to design an effective in vivo contrast agent, and the versatility of dye doped silica nanoparticles is of particular relevance to this goal [30].

This multifluorophoric structure can present complex photophysical properties—multiple emissions with multiexponential decays—which can sometimes

also be affected by the environment. On the other hand, a proper design can induce cooperative behaviours among some or all fluorophores in each nanoparticle, interpreting amplification effects (the status of one dye affects the properties of all the neighbouring ones) and other advantages as an increase of brightness and a decrease of noise. All these beneficial features arise thanks to the interconnection of the fluorophores within one nanoparticle which allows efficient energy transfer phenomena such as Förster Resonance Energy Transfer—FRET—which involves the deactivation of the donor excited state and the excitation of that of the acceptor [31, 32]. Homo-FRET can indeed be used to distribute the excitation energy among a variety of dyes. Competitive energy transfer pathways can be created and the fastest can induce a predictable direction of energy migration. All this is possible only after proper design of the interfluorophoric distances (FRET is proportional to r^{-6}) and a suitable choice of luminescent species to be mixed which should have appropriate photophysical properties (FRET is proportional to the overlap integral J which describes the matching between emission of the donor and absorption of the acceptor in terms of energy and probability) [33] (Fig. 3). One of the great strengths of FRET is that in a well-designed system many different consecutive, cascade, or independent FRET events can take place, both in organized and non-organized nanoobjects [34]. This multiple energy migration involves a very directional event or, on the other hand, the photophysical properties of the whole device. A very important point to bear in mind is that FRET can allow the creation of a species with very high pseudo-Stokes shift, a powerful tool to obtain NIR emitting probes [35].

Therefore the presence of a single kind of dye or of different emitting species as neighbours in a single nanoparticle can lead to diverse properties and also to collective behaviours which can be exploited to obtain ultra-bright species suitable for high sensitivity applications such as in vivo optical imaging.

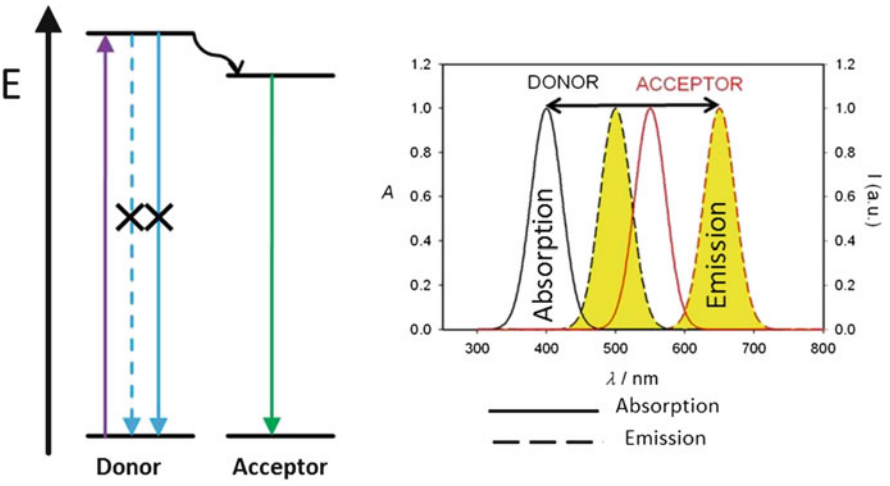

Fig. 3 Energetic scheme of FRET and of the induced pseudo-Stokes shift

Many interesting results, in fact, have already been obtained with nanoparticles containing only one kind of photophysically active species [36], and elegant systems have been prepared to address crucial problems advantageously, such as the mapping of sentinel lymph nodes [37, 38]. However, we strongly believe that luminescent silica nanoparticles doped with different dyes featuring collective processes make these nanostructures even more attractive. In this review we intend to underline these aspects, presenting selected examples to describe the state of the art of these materials as contrast agents in optical imaging and optical sensing.

We start with a very summarized discussion of the synthetic methods where the reader mainly finds a sketch of the rationale and goals of the preparation and relevant references for a wider dissertation of the subject. The reported examples are gathered in two chapters focussing on (1) nanoparticles containing different kinds of dyes and (2) luminescent nanosensors. As already mentioned, this work has no ambition to be exhaustive but we aim to give the interested readers a feeling of the progress in the area from a viewpoint that we hope stimulates the creativity and curiosity of researchers in the field.

2 Synthetic Strategies

Fluorescent silica nanoparticles (NPs) are powerful tools able to work as labels [8, 39] and sensors [40], usually obtained by means of wet sol-gel synthetic approaches characterized by simplicity, low costs, versatility and control over NP dimensions.

The first synthesis of highly monodisperse silica NPs was described by Stöber [41], who used tetraorthosilicate (TEOS) hydrolysis and condensation catalyzed by ammonia in a water-alcohol mixture to form silica NPs. Lately this strategy has been implemented by Van Blaaderen [41, 42] who obtained fluorescent silica NPs covalently doped with fluorescent dyes endowed with alkoxysilane groups, and more recently, by other groups who developed some interesting variations based on biphasic reaction media [43] and on heterogeneous nucleation processes [44].

The Stöber–Van Blaaderen method is straightforward for its simplicity, it supplies highly and stable monodisperse NPs in a wide dimensional range (~20 to 800 nm—with one pot procedures), and is applicable to many ethanol soluble organic dyes. These colloidal particles are stabilized by the electrostatic repulsion between the siloxane groups of the NPs surface, and the presence of these groups can be used for the introduction of functionality for biomolecule targeting. NPs surface functionalization is the major weak point of this synthetic approach because surface modification can be hampered by aggregation and loss of the pristine colloidal stability of the system, especially when tiny NPs are concerned.

The reverse microemulsions strategy (water-in-oil) [45] exploits the same hydrolysis and condensation processes of the previous method, but with chemical reactions that are confined in the water nano-pools of a reverse microemulsion, made of an isotropic mixture of a surfactant, water, and a hydrocarbon (usually

cyclohexane). This approach is extremely versatile for obtaining functionalized NPs, because the addition of the reagents to produce the core and a functionalized shell can be made in sequence without intermediate purification procedures, reducing the possibility of aggregation. With surface functionality introduced to reduce non-specific binding and aggregation, NPs can be efficiently recovered and purified from the microemulsion by repetitive precipitation and washing steps. The strongest limitation to water-in-oil strategies is that they are exclusive to water soluble and, preferentially, positively charged dyes: this is why the most used dye with this approach is $Ru(bpy)_3^{2+}$.

An alternative and more recent strategy employs micellar aggregates or co-aggregates in water as self-organized templates to confine the silica NPs growth: such approaches are reported as direct micelles-assisted methods [46–48]. Because silica precursors such as TEOS or other organo-alkoxysilanes, and indeed the majority of the organic dyes, have a lipophilic nature, they can be efficiently entrapped in self-organized templates with a lipophilic core. When an organosilane (for example VTES, triethoxyvinylsilane, APTES, 3-aminopropyltriethoxysilane) are used together with a low molecular weight surfactant (AOT, bis(2-ethylhexyl) sulfosuccinate sodium salt, Tween 80) in the presence of ammonia, these NPs systems have often been referred to as ORMOSIL (ORganic–MOdified–SILica).

Prasad and coworkers made the greatest contributions in the field. These NPs, with a diameter spanning in the 20–30 nm range and a mesoporous silica matrix, were suitable for PDT applications [49], with dyes that usually need to be linked covalently to the nanoparticles to avoid leaching [50, 51]. Targeting and labelling capabilities for conjugation with bioactive molecules [52] were obtained with functionalization with alkoxysilane bearing groups such as $–NH_2$, –COOH, and –SH by means of contiguous synthetic strategies, NPs were obtained functionalized with PEG [53], or by incorporating QDs [54] and Fe_3O_4 nanoparticles [55].

Hexadecyltrimethylammonium bromide (CTAB) micelles were used by Wiesner and coworkers to develop tiny mesoporous PEGylated NPs (6–15 nm): this approach allows control of the NP morphology, which depends on the number of micellar aggregates entrapped in each nanoparticle during the silica core formation [56].

A different synthetic possibility is to synthesize cross-linked micellar NPs featuring core-shell structures [46, 57]. This direct micelle-assisted strategy employs high molecular weight surfactants, such as Pluronic F127, F108, or Brij700 [58], or bridging organo-silane precursors [59]. The presence of self-organized templates and of condensation processes which are promoted in acidic environment makes these synthetic approaches quite different from the Stöber method. TEOS condensation is promoted by acids such as HCl [59] or HOAc [60] in a set of conditions ($pH < 4$) in which the hydrolysis process is faster than condensation—a situation that promote the formation of Si–O–Si chains which finally undergo cross-linking [61, 62]. During the NP formation, silica is confined in the micellar environment, and these surfactants undergo entrapment–adsorption processes, with the valuable consequence of NP surface modification in a one-pot procedure.

Pluronic F127, characterized by a tri-block PEG-PPO-PEG (poly (ethyleneglycol)-poly(propylene oxide)-poly(ethylene glycol), MW 12.6 KDa) structure and quite large micellar aggregates in water (~22 to 25 nm), is probably the most versatile surfactant for this synthetic approach and our group had a leading part in the development of fluorescent NPs obtained by Pluronic F127 micelles-assisted method (PluS NPs, Pluronic Silica NanoParticles) [39, 63]. The PPO inner core of these aggregates enables the use of TEOS as silica precursor, contributing to a more stable and dense silica network compared to ORMOSIL NPs. Great versatility is conferred by the possibility of using many alkoxysilane derivatized dyes—from polar to very lipophilic—which can be entrapped in the silica network under mild acidic conditions.

Their core-shell structure presents a hard diameter of 10 nm and an average hydrodynamic diameter of ~25 nm: the morphological properties were verified by TEM and DLS (Dynamic Light Scattering) [57], AFM measurements [46], and ^{1}H-NMR, showing the orientation of the Pluronic F127 PEG chains. TGA (Thermo Gravimetric Analysis) analysis performed on samples subjected to ultrafiltered samples also showed the stable linking between the surfactant and silica core [64]. PEGylated core-shell NPs are very monodisperse in water and physiological conditions, where they show low adhesion properties towards proteins and prolonged colloidal stability. Their versatility has been exploited in many fields: photophysical studies [57, 63], sensors [40, 65], biological imaging [60], fluorescent-photoswitchable nanoparticles [66], self-quenching recovery [34], and ECL [46, 64].

For applications involving labelling [67] or non-specific targeting [68], the functionalization of these NPs was achieved acting on the Pluronic F127 hydroxy end groups. We found that cellular uptake was influenced by PluS NPs functionalization, with cytotoxicity that was negligible towards several normal or cancer cell types, grown either in suspension or in adherence [68], for PEGylated NPs presenting external amino or carboxy groups. We recently exploited the core-shell nature of these NPs to develop NIR fluorescent NPs for regional lymph nodes mapping [37]. We synthesized negatively charged NPs having programmed charges positioning schemes to influence their biodistribution for lymph nodes targeting in vivo. We found that NPs having negative charges in the mesoporous silica core—hidden by a PEG shell—demonstrated a more efficient and dynamic behaviour during lymph nodes mapping. This last example showed once again the versatility of the core-shell silica-PEG structure, where the modifications of both core and shell parts play a synergistic effect in defining the efficiency of the fluorescent probe.

We have found that for in vivo imaging a fundamental requisite is the absence of dye leaching from the NP towards the biological environment, because this compromises the overall signal-to-noise ratiomaking fruitless the brightness increase produced by a nanoprobe. Trialkoxysilane derivatized dyes [69] can be synthesized efficiently to ensure condensation within the silica matrix, a critical issue, especially for NPs of dimensions lower than ~50 nm, characterized by a very high surface to volume ratio.

3 Multifluorophoric Doping of Silica Nanoparticles

As already anticipated in the introduction, even though dye doped silica nanoparticles are increasingly studied as contrast agents for fluorescent imaging, their clinical application is still only theoretical and further steps forward are needed in that direction. In our opinion, this process could be accelerated and facilitated by the optimization of FRET in multiple-dye-doped nanoparticles [33] because this could facilitate the preparation of materials with two very valuable characteristics: (1) NIR absorption and emission, and therefore suitable for biomedical application; (2) nanoparticles suitable for multiplexed analysis.

NIR excitation and emission are, in fact, extremely beneficial in the biomedical field but NP doping with a single NIR emitting dye has many drawbacks intrinsically relating to the nature of this class of emitters, typically characterized by very small Stokes shifts and quite low luminescence quantum yields. In such systems, high background signals are common, mostly caused by interference of the excitation light.

One of the most versatile and convincing strategies to overcome this problem and to obtain novel and customized photophysical properties is the design and activation of proper energy transfer events which take place only when a high local density of dyes is reached. The distance between the donor and the acceptor needs to be typically <10 nm for fast and efficient energy transfer events to occur, and therefore the segregation of many and different dyes in the same nanoparticle is a straightforward way to obtain suitable separation between them. This strategy can also lead to the formation of excimers and aggregates but homo- and hetero-FRET can have a synergistic role as shown in the following discussion.

Moreover, the need for cheaper and more rapid diagnostic protocols is a well-established implementation goal for current diagnostic strategies which are not always able to fulfil the time constraint imposed by some kinds of pathologies, and the use of NPs for multiplexed analysis, that is to say for simultaneous multi-analytes detection, can be an efficient answer.

A recognized advantage of silica nanoparticles is that they can be easily modified in different ways accordingly to the strategy in mind. In this context, Tan and co-workers have explored and proposed some very interesting nanoarchitectures. In a first example [70] they have developed aptamer-conjugated nanoparticles to detect (and extract with the help of magnetic nanoparticles) three different lymphoma cells in a single analysis. With this aim they used three diverse high-affinity DNA aptamers for recognition, each bound to a different fluorescent silica nanoparticle ($d = 50 \pm 5$ nm) doped with $Ru(bpy)_3^{2+}$, tetramethylrhodamine, or Cy5, respectively. The same authors later proposed a more elegant approach, allowing a higher multiplexing ability, based on FRET for multiplexed bacteria monitoring and imaging [71] (Fig. 4). In this work they prepared silica nanoparticles doped with a combination of up to three kinds of dyes (fluorescein, rhodamine 6G, and 6-carboxy-X-rhodamine) in different doping concentrations. In these conditions only a partial energy transfer occurred between the dyes and this allowed for the

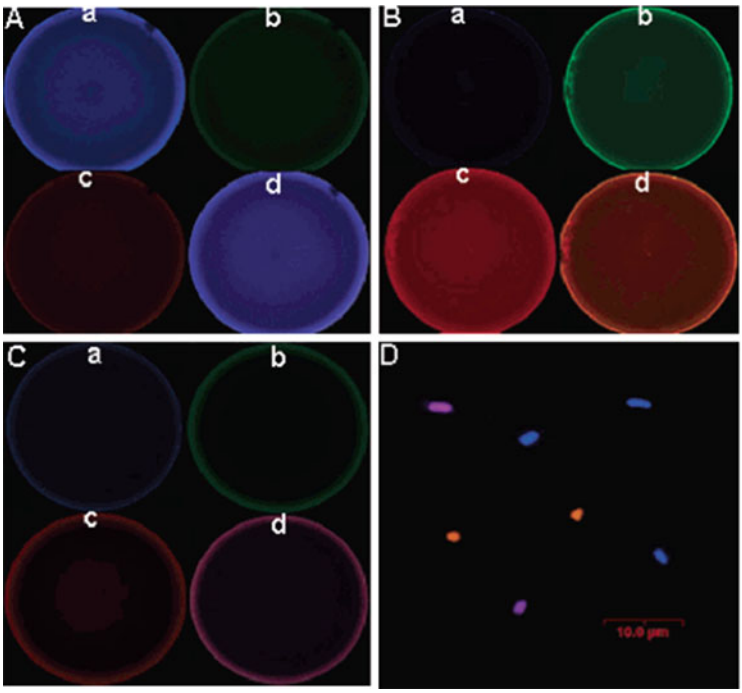

Fig. 4 (A-C) Fluorescence images of three types of FRET NPs taken under a confocal microscope: (**a**) FAM emission channel; (**b**) R6G emission channel; (**c**) ROX emission channel. (**d**) Combinatorial colour of the three channels. The three types of NPs exhibit *blue*, *orange* and *purple colours*. (D) Confocal image of three bacteria species specifically covered with the corresponding antibody labelled NPs (copyright Wang et al. [71])

detection, under a single excitation wavelength, of a number of bands equal to the number of doping fluorophores [72]. Their intensities could be controlled by varying the doping degree and ratio of all the luminescent species to obtain a large library of bar-coding NPs, thereby allowing the simultaneous detection of many bacterial pathogens or cancer cells [73]. The data collected in these papers show how this approach brings important advantages: (1) the simplification of the experimental setup needed for their detection because a single laser source was needed for their excitation; (2) the high specificity provided by the aptamers and the nanoparticles brightness could potentially remove the need for sample enrichment and amplification steps, allowing a fast diagnosis at the earliest stage of a disease.

K. Wang and co-workers [74] have also studied similar systems with silica nanoparticles (50 nm diameter) obtained via the microemulsion method and non-covalently doped with a tris-bipyridyl ruthenium complex and methylene blue units. Their main goal was to obtain a very large (around 200 nm) Stokes shift to prepare suitable fluorescent NPs for small animal in vivo imaging.

In this same framework, we have proposed Plus NPs that can be used as a scaffold to organize and to connect molecular components electronically

[57]. These very monodisperse water-soluble silica core-surfactant PEG shell nanoparticles (Plus NPs) were covalently doped in the core with a Rhodamine B derivative although, exploiting simple hydrophobic effects, a second luminescent species (Cy5) was adsorbed in the shell. These NPs could hence simultaneously behave as fluorescent labels (for imaging applications) and as carriers for the delivery of hydrophobic compounds (drugs). Moreover, the efficient communication via a partial ET between the active molecules trapped in the core and the hosted species in the shell was demonstrated experimentally.

Starting from these very promising results we have proposed two systems based on co-doping with two different fluorophores of the silica core of nanoparticles to obtain modular nanosystems for in vivo optical imaging with the goal of future use in clinics [60, 67]. The Plus NPs of both studies were doped with a cyanine and Rhodamine B in the core, the main difference being that one system was decorated on the outer shell with peptides able to target the hepatic cancer cells specifically [67] whereas the other non-targeted one was used to investigate the non-specific distribution and circulation of these materials in vivo [60]. The injection of the first nano-contrast agent in a mouse proved that the functionalization of the NPs with metastasis-specific peptides took to their homing and accumulation in the target tissues, resulting in specific visualization even of sub-millimetric metastases. In this system the energy transfer between the two doping fluorophores is partial, allowing the detection and acquisition of the emission signals of both of them (Cy5 and Rhodamine B). The comparison and superimposition of these images allowed for background subtraction and signal amplification, resulting in the enhancement of the imaging sensitivity. It should be noted that this is a modular approach, providing great versatility in achieving cancer cell-targeted delivery of a number of therapeutic, diagnostic, or teragnostic compounds.

In the second system [60] we wanted to use a single bio-label for both in vivo imaging and ex vivo microscopy on the same animal. A partial energy transfer between the two dyes maintains both signals, for in vivo experiments (NIR region, Cy7 derivative) and tissue investigations with optical microscopes equipped with light sources and detectors operating in the visible region (rhodamine B). In our nanoparticles it was possible to observe an efficient sensitization of the cyanine but also a residual 25% of luminescence of the rhodamine, sufficient for a high signal at the optical microscope, allowing the proposed goal of performing in vivo and ex vivo experiments with the same NP on the same animal to be achieved. It should be emphasised that this cannot be achieved with QDs or metallic NPs, because typically their one colour emission is tuned by their shape and dimensions.

Taking advantage of these results, we have then tried to exploit this modular and very versatile approach to optimize the system further for in vivo imaging [35]. Neighbouring Cy5.5 and Cy7 dyes in different ratios—both covalently linked in the 10 nm diameter core of the Plus NPs—led to a very sensitive contrast agent with high brightness in the NIR. Interestingly, the mixing of two different dyes advantageously led to a decrease the efficiency of the self quenching processes observed in single dye doped NPs, further increasing the brightness of the system. Small-animal in vivo imaging experiments have shown very promising results, indicating the great potential of nanoparticles realized with this approach (Fig. 5).

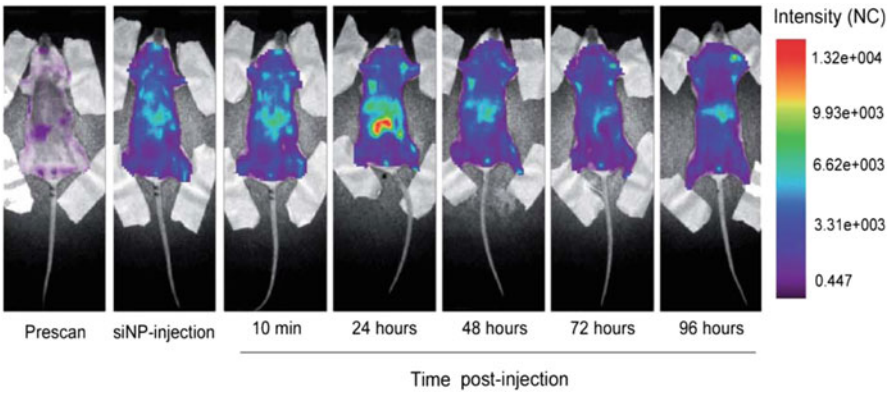

Fig. 5 Whole-body scan of a representative mouse in supine position; fluorescence intensity images were acquired at the indicated time post-injection and are displayed in normalized counts (NC). BALB/c mice were injected intravenously via the tail vein with 1 nmol of NPs and analyzed by optical imaging (copyright Biffi et al. [35])

We have discussed so far silica nanoparticles with multi-fluorophoric doping with two or more kinds of dyes able to give only partial FRET; it is important now to highlight that complete energy transfer in similar systems could represent a very valuable feature, allowing an increase in the number of analytical approaches towards the detection of many species via very bright, NIR emitting species. In spite of the brilliant and pioneering work of Tan and co-workers, an almost complete energy transfer in multi-doped silica nanoparticles had not been achieved until very recently, when we decided to exploit the particularly favourable characteristic of the Plus NPs to optimize these processes and prepare brighter contrast agents for medical imaging.

The first problem to overcome to enhance brightness in nanoparticles is to contrast the detrimental effects of self-quenching on the luminescence quantum yield, a very common feature when large amounts of dyes are present in a small volume. In these conditions, in fact, when the absorption cross section is additive, the luminescence can be negatively affected by their proximity, imposing a limit on doping degree to a relatively low number of luminescent units. We have proposed an alternative approach exploiting the efficient homo-FRET to boost the hetero-FRET towards highly luminescent energy acceptors [34]. We prepared PluS NPs doped in the core with approximately 40 coumarin dyes per NP, and with a bodipy that was chosen as energy acceptor because its quantum yield and spectral properties are not affected by neighbouring coumarin units. We found that a few molecules of acceptor (around 5) could very efficiently collect the light absorbed by all the coumarins via such a highly efficient energy transfer. Importantly, because of the high rate constant associated with this process, the self-quenching was almost completely prevented, and almost no loss of the excitation energy could be detected. The straightforward consequence is the linear increase of the brightness as a function of the coumarin molecules present in the NPs, allowing an unprecedented brightness (Fig. 6).

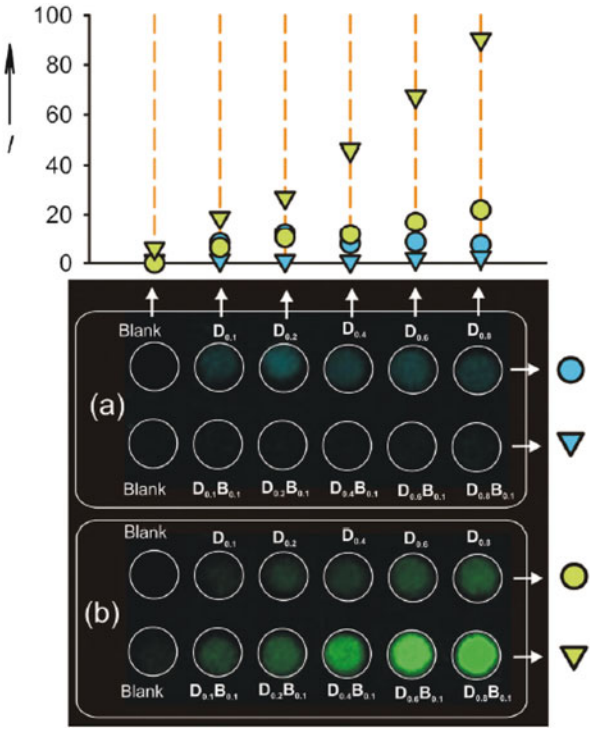

Fig. 6 Fluorescence images of a set of 12 wells containing dispersions of the NPs in water ($c = 1 \times 10^{-7}$ M), as detected with either a *blue* (**a**, $\lambda_{em} = 460$ nm) or a *green* (**b**, $\lambda_{em} = 530$ nm) *filter*. The total intensity determined by the integration of each spot is plotted in the *top graph* (copyright Genovese et al. [34])

Moreover, this system also presents the valuable advantage of a greater pseudo-Stokes shift which is produced by the wavelength difference between the maxima of the donor absorption and of the acceptor emission.

After experimentally proving that this strategy is general and limited only by the photophysical properties of the fluorophore couples, which must be suitable to allow an efficient FRET, we have tried to push the system further towards larger and larger separations between the excitation and emission maxima. Our goal was to obtain high luminescence in the NIR region, but also a very high signal-to-noise ratio, thanks to the reduced interferences from Rayleigh–Tyndall and Raman bands. We have therefore prepared and characterized multi-fluorophoric PluS NPs, each containing up to four different kinds of fluorophores [35], and we could observe unprecedented efficiencies (higher than 94%) in the ET processes in the doping dyes (a sort of cascade ET). This leads to a very large and tuneable pseudo-Stokes shift (up to 435 nm) for each NP which is also characterized by a single colour emission (that of the reddest dye of the four, the final acceptor) with a negligible residual emission intensity from all the donor dyes, and a very high brightness, even

exciting the "bluest" donor. These multicomponent PluS NPs can thus be seen as very promising materials for multiplex analysis in medical diagnostic techniques.

We conclude this section by discussing an example of silica multi-dye nanoparticles designed as possible theranostic agents. S. R. Grobmyer and co-workers have proposed mesoporous silica nanoparticles around 110 nm in diameter as theranostic platforms for bioimaging and cancer therapy [75]. They first covalently doped these species with a properly silanized cyanine (IR780) which, after derivatization and incorporation, showed a highly enhanced luminescence quantum yield (>300-fold) and Stokes shift (>110 nm). In a second step they also loaded a Si-naphthalocyanine in the pores of the NPs. After the optimization of both dye concentrations, the resulting multi-dye structures, thanks to a partial energy transfer, allowed the imaging of a murine mammary tumour in vivo after intratumoral injection and then its photothermal ablation via laser irradiation. The non-fluorescent metallo-naphthalocyanine, in fact, acts as a rather efficient photothermal therapeutic agent as first evidenced by bioluminescence analysis and then proved by the histological analysis. The same authors have also proved that these NPs remain within the tumour for several days and are suitable for successive activations, allowing the application of image-guided fractionated photothermal ablation.

A second aspect to be carefully evaluated and addressed is the clearance time, the fate of these imaging or theranostic agents being still mostly unknown, although it is a fundamental aspect that needs to be clarified before considering any possible clinical translation. The multi-dye bright NIR absorbing and emitting nanoparticles described in this chapter can, in our opinion, be a key tool in making significant steps forward in this area, allowing NPs tracking in vivo in real time via fluorescence imaging.

4 Luminescent Chemosensors Based on Silica Nanoparticles

Luminescent chemosensors have already found wide applications in many fields of great economic and social importance, such as environmental monitoring, process control, and food and beverage analysis. In addition, thanks to the high sensitivity and the high spatial and temporal resolution granted by luminescence [76–78], fluorescence-based chemosensors can enable the investigation of the functions and possible misregulation of crucial target analytes in living systems [79, 80], especially at the cellular level. To face the latest challenges of biology and medicine, however, very sophisticated systems are needed, and this is the reason why nanostructured architectures are so widely studied in this context. In particular, silica nanoparticles can offer many advantages compared to their molecular and supramolecular counterparts together with the above-mentioned high brightness and photostability.

The first is related to the possibility of engineering collective energy- and electron-transfer processes which, if designed to modify the luminescence properties of several dyes upon a single complexation event, can lead to large signal amplification effects and thus lower detection limits [76]. Moreover, as discussed in the previous section, collective energy-transfer processes can also lead to an even higher brightness and a very large Stokes shift (up to hundreds of nanometres), thus minimizing the interferences coming from the scattered light, the Raman band, and the auto-fluorescence of the biological sample.

Another advantage is the possibility offered by silica nanoparticles to obtain ratiometric systems easily. Quantitative intensity measurements using fluorescent chemosensors can indeed be affected at a single wavelength by their dependence not only on the concentration of the analyte but also on the concentration of the chemosensors itself and, possibly, on the optical path and on environmental conditions. This problem can generally be overcome by using time-resolved techniques or by properly designing the system to be able to compare the signals coming from two different bands. Using silica nanoparticles, this can be achieved by inserting a fluorescent probe together with an analyte-independent fluorophore in the silica-based nanosensor. The most common methods use a design that aims to prevent all electronic interactions between the two fluorescent units, thus eliminating the possibility of energy transfer processes. Typically, the reference dye is included in the core of the nanoparticles, whereas the probe is inserted in an outer shell or bound to the surface [79, 81].

Moreover, using DDSNPs, the solubility and stability of the system in solution is conferred mainly by the silica structure; in this way, many interesting compounds that, because of their limited solubility, cannot be used in an aqueous environment can instead be conveniently inserted in the DDSNP structure and also work in water [82–84]. In these cases, however, we recommend that the possibility be considered that the photophysical properties of the chemosensor in its free form and/or when interacting with the analyte could be drastically changed when inserted into the silica matrix based on what is observed in aqueous or organic solvents. At the same time, the affinity towards the analyte can also change because of the insertion of the chemosensor into the silica matrix. Because of cooperative effects, a considerable affinity increase can usually be obtained, which can be used to push their sensitivity to even lower levels. Interestingly, we have also proved that even the stoichiometry of complexation of a chemosensor can be changed when inserted inside a DDSNP [83].

In biology the ideal probe should allow precise compartmentalization, without perturbing the equilibrium present in the cell, for example not depleting cellular ion pools when detecting metals [85]. To achieve this, a high signal-to-noise ratio and a suitable affinity and selectivity are, for a chemosensor, mandatory. In addition, the possibility of derivatizing the DDSNPs with suitable biomolecules can help to increase selectivity towards a specific hat can be acquired cellular compartment, improving the information acquirable by the system [85].

To date, the use of fluorescent probes based on silica nanoparticles for cell imaging has been reported for determining the concentration of protons (pH), metal

ions (with a possible future extension to their speciation), anions, small molecules (including molecular oxygen), reducing agents (such as glutathione), and enzymes. We have selected here few examples with the aim of showing the best features of silica nanoparticles and their possible future developments.

4.1 pH Probes

Tissue acidosis is a clear indication of inflammatory diseases, and low pH values have been found, for example, in cardiac ischemia and inside and around malignant tumours [86]. For this reason, although pH chemosensors are, at least in principle, among the simplest, their full development is of particular interest. In this regard, it is important to mention the pioneering work of Wiesner and coworkers [87] who, based on the Stöber strategy, designed a core/shell architecture. In particular, the silica core was doped with the reference dye, a conjugate of tetramethylrhodamine, whose fluorescence properties do not depend on pH over a large range (Fig. 7a). The outer silica shell was instead doped with fluorescein, which assumes different pH-dependent equilibria; of particular importance between the monoanionic and dianionic forms ($\Phi = 0.36$ and 0.93, respectively; $pK_a = 6.4$).

The ratiometric pH response of the two signals were used to prepare a calibration curve (Fig. 7b). The nanoparticles were than internalized in RBL-2H3 cells, and it was possible, after correction for taking into account a certain amount of autofluorescence, to measure the pH in different compartments (from 6.5 in early endosome to ca. 5.0 in late endosome/lysosome). Many examples of fluorescent NPs designed for pH sensing have since been reported. A similar couple of dyes (fluorescein as the pH sensitive dye and Rhodamine B as the reference dye), grafted to mesoporous silica NPs, were used by Chen and coworkers [88]. These authors used two differently charged ethoxysilane derivatives to functionalize the NPs surface and observed how the charge influenced the final location of the NPs in HeLa cells. In particular, positively charged NPs were found to prefer higher pH regions (mostly cytosol) whereas negatively charged NPs accumulated in acidic endosomes. It should be noted that, as expected, the internalization of the NPs also depends on their charge.

Doussineau and coworkers [89], for example, prepared NPs with a diameter of 100 nm, again containing rhodamine as a reference and, as a pH probe, a fluorescent naphthalimide derivative grafted to the NPs surface through linkers of different lengths. The two-dye structure showed good pH sensitivity in a physiologically relevant pH range with an ON–OFF response of the naphthalimide units. Wang and coworkers prepared another, smaller (diameter 42 nm) ratiometric system, able to sense pH changes in a range between 4 and 7 in murine macrophages and in HeLa cells during apoptosis [90]. In this case the NPs were doped with the tris(2,2′-bipyridyl)ruthenium(II) complex as reference and with a fluorescein derivative. The changes in lysosomal pH were monitored in real time after exposure to the antimalaria drug chloroquine. Ratiometric fluorescence detection allowed the

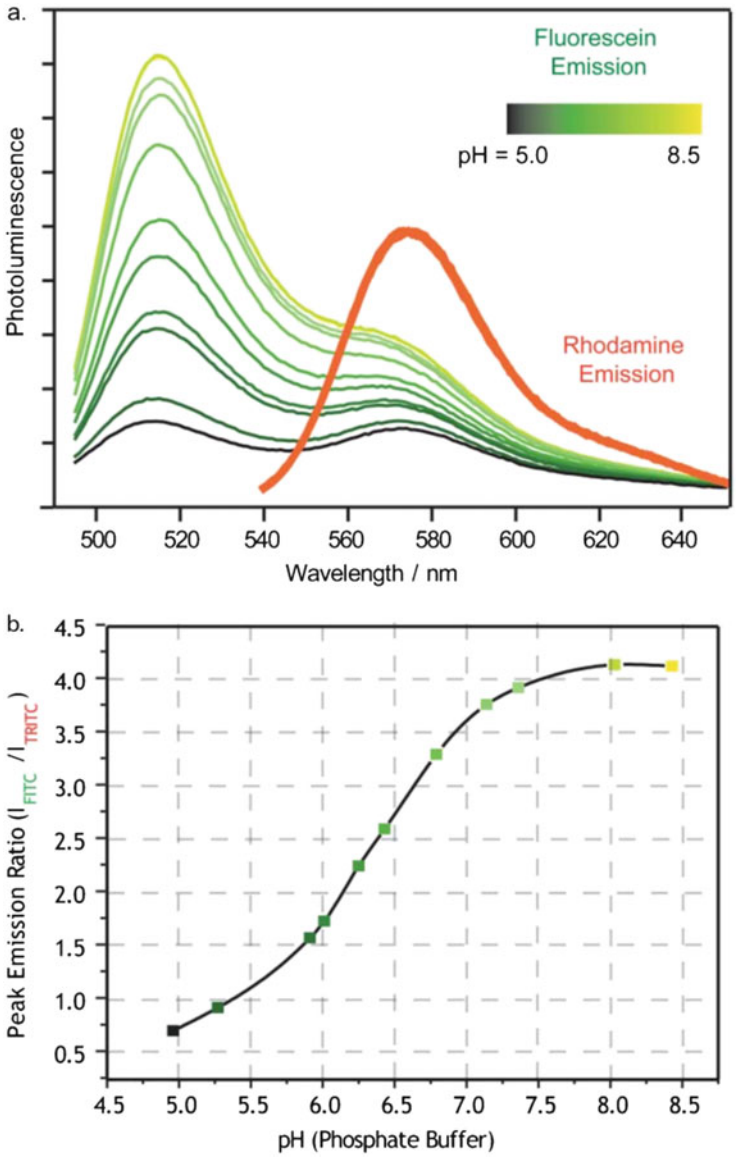

Fig. 7 (**a**) Spectrofluorometry data for 70 nm dual-emission core-shell fluorescent silica nanoparticle pH sensors showing fluorescein (*green*) and TRITC (*red*) in phosphate pH calibration buffers from pH 5–8.5. (**b**) A ratiometric calibration curve based on the peak intensity ratio between fluorescein and TRITC across the pH range under investigation (reproduced, in part, with permission from Burns et al. [87])

authors to conclude that chloroquine stimulates lysosomal pH changes. Upon incubation of HeLa cells with the same nanosensors, it was instead possible to observe, in real time, intracellular acidification in apoptotic cancer cells after treatment with dexametasone, a synthetic glucocorticoid commonly used as an anti-inflammatory agent.

A possible strategy to obtain a higher sensitivity can be developed, based on trying to maximize the signal changes under the same pH change. This approach has been used by Shoufa Han et al. [91], who doped mesoporous silica nanoparticles (diameter 100 nm) with fluorescein (whose fluorescence, as we have already discussed, decreases in acidic media) and the acid activable Rhodamine 6G lactam, whose fluorescence increases with decreasing pH. Because the two signals change in opposite directions, small pH changes can induce large variations in the ratio between the two intensities. It was possible in this way to monitor lysosomal pH in live L929 cells.

4.2 Ion Chemosensors

After pH, the Cu^{2+} probes are the most studied chemosensors based on silica nanoparticles. This research trend can be easily explained by considering the ability of this ion to form stable complexes and to perturb dramatically (typically, quenching) the fluorescence properties of the dye, together with the importance of copper ions in environmental and biological matrices. A very interesting example is represented by the derivatization of mesoporous silica (SBA-15) with a 1,8-naphthalimide-based receptor [92]. In aqueous solution, Cu^{2+} quenched the fluorescence of 1,8-naphthalimide with high efficiency and selectivity (detection limit 0.01 μM), with Hg^{2+} being the most important interfering species. Interestingly, the same receptor, but conjugated with a treholose unit to confer the right water solubility to the system, showed a ratiometric response towards copper ions, without an appreciable interference by mercury ions. In vitro (MCF-7 human breast cancer cells) and in vivo (5-day-old zebrafish) experiments showed in both cases the internalization of the nanostructures and a strong quenching of the fluorescence after incubation with Cu^{2+} ions. In a second example, the recognition was achieved by capping silica nanoparticles having a diameter of 10 nm with a trialkoxysilane derivative of fluorescein bearing two carboxylic functions as coordinating sites [93]. The fluorescence of this nanosensor showed a selective and reversible (upon addition of EDTA) quenching in the presence of copper ions in water at pH 7.4, affording an interesting detection limit of 0.5 μM. Furthermore, this nanoarchitecture was able to permeate into HeLa cells, and its fluorescence decreased, as expected, when the cells were incubated with Cu^{2+}.

Copper(I) is also a crucial species to monitor inside cells, and plays a role, among others, in neurodegenerative diseases. In this framework we have developed a ratiometric chemosensor based on core-shell silica NPs (Fig. 8) [65], synthesized using Pluronic F127 as a template and doped with a coumarin derivative.

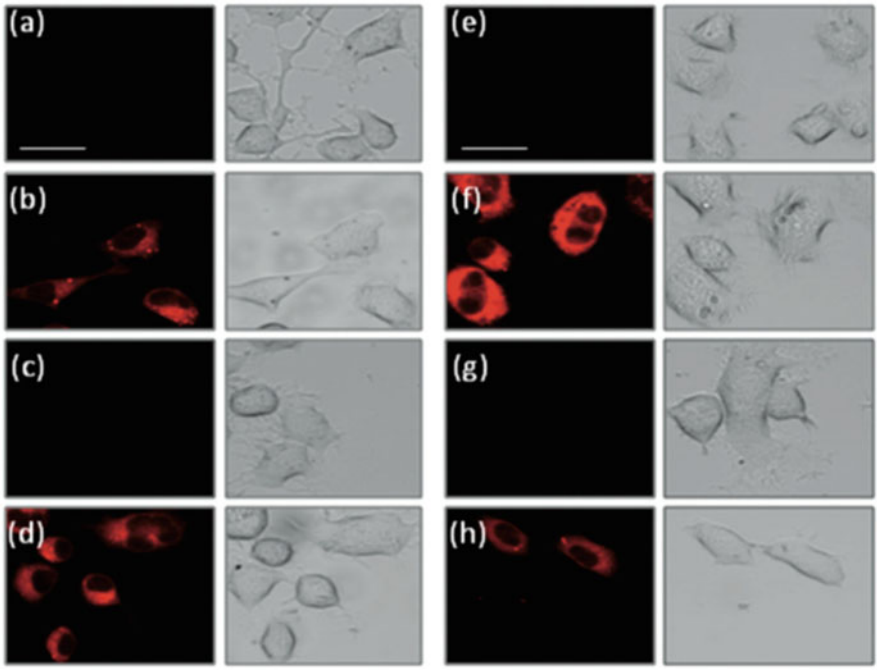

Fig. 8 Confocal microscopy emission ($\lambda_{ex} = 543$ nm; $\lambda_{em} = 572$ nm) and corresponding bright-field images for the SHSY5Y cell line: (**a**–**d**) cultured in DMEM medium for 24 h, and (**e**–**h**) supplemented with $CuCl_2$ (100 mm) for 5 h, incubated at 378 °C. The probe treatments (5 min incubation at 25.8 °C, then rinsed with PBS) are as follows: (**a**, **e**) control PBS; (**b**, **f**) molecular sensor (5 μM); (**c**, **g**) nanoparticles (5 μM); (**d**, **h**) sensor inside NPs (5 μM; 1:1 molar ratio); *scale bar*: 30 mm (copyright Rampazzo et al. [65])

The addition of the selective probe designed by Chang et al. [94] to a water dispersion of the NPs leads, because of its lipophilic nature, to its inclusion into the nanostructure, making possible an efficient energy transfer process between the coumarin dye bound in the silica matrix and the bodipy of the probe located in the shell close by. The complexation of Cu^{+} by the probe led to changes in the absorption and luminescence properties of the bodipy which affected both the coumarin signal (because of a change in the efficiency of the energy transfer process) and the bodipy signal (because of the change in its fluorescence quantum yield).

This resulted in a ratiometric system with an amplified response. We were also able to demonstrate that the inclusion of the probe led to a tenfold increase of its affinity towards the target analyte. Experiments conducted in SHSY5Y cell lines also confirmed the validity of this approach for biological systems. For these reasons, we strongly believe we could significantly push further the application of chemosensors in biomedical analysis, considering that it enables the use of otherwise water insoluble species without demanding synthetic efforts.

In the development of chemosensors, the design of efficient systems for monitoring the concentration of anions has been typically quite challenging. In this context, it is relevant that the example reported by Bau et al. [95] involved the preparation of a ratiometric probe for chloride anions based on silica NPs grafted with 6-methoxyquinolinium as the chloride-sensitive component and fluorescein as the reference dye. The measured Stern–Volmer constant was 50 M^{-1} at pH 7.2, sufficient to monitor chloride ion changes around physiological concentrations. In fact, these nanostructures were able to penetrate neuronal cells at submillimolar concentrations and to signal in real time chemically induced chloride currents in hippocampal cells.

4.3 Probing Molecular Processes

Interestingly, silica nanoparticles can also be used with biological processes. In particular, the possibility of following the triggering of apoptosis, programmed cell death, has attracted the attention of several researchers. Malfunctioning apoptosis can, in fact, lead to several pathological conditions, such as neurodegenerative disorders, cardiovascular diseases, and cancer. A popular extracellular method for the detection of apoptosis involves monitoring the distribution of phospholipids on the cell surface; in particular, the appearance of phosphatidylserine (PS), which usually constitutes less than 10% of the total phospholipids in cell membranes, on the outer part of cell membranes is a universal indicator of the initial stage of apoptosis.

Yeo, Hong and coworkers have grafted to the surface of silica nanoparticles doped with $Ru(bpy)_3^{2+}$ the phenoxo-bridged Zn(II)-di-2-picolylamime complex (pbZn(II)-DPA, Fig. 9), which selectively recognizes PS among the different animal-cell-membrane phospholipids [96].

Interestingly, the authors showed through fluorescence microscopy that Jurtkat T cells were not stained by the nanoparticles except when treated with camptothecin,

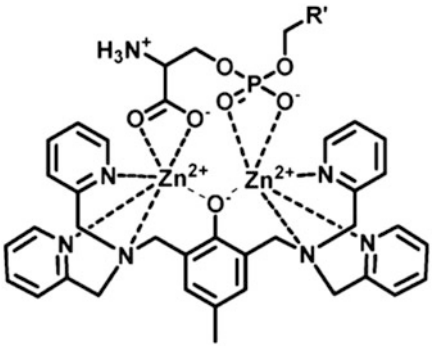

Fig. 9 pbZn(II)-DPA complex

an apoptosis inducer. Of note, the orange luminescence of the nanoparticles was localized on the cell surface, as expected in the case of binding to externalized PS.

A different example of monitoring apoptosis is to follow the activity of caspases, a family of cysteine proteases which play critical roles in this process. Lee, Chen and their colleagues prepared a very interesting nanosensor which made possible the multiplex imaging of intracellular proteolytic cascades [97]. The design of this nanosensor is very elegant (Fig. 10). Mesoporous silica nanoparticles, with a diameter of 60 nm, were doped, after their suitable derivatization with a silane group, with three different kind of commercially available molecules belonging to the series of the so-called black hole quenchers (BHQ) which, having large and intense absorption bands in the visible region of the spectrum, can efficiently quench the fluorescence of many kinds of organic dyes through a FRET mechanism.

The nanoparticle surface was grafted, through a short PEG spacer, with specific substrate (an oligopeptides) for caspase-3 derivatized with a fluorophore (Cy5.5GDEVDGC). The fluorescence of Cy5.5, because of the efficient quenching of BHQs, was strongly reduced (up to ca. 360-fold, depending on the doping degree). Incubation with caspase-3 led to a strong fluorescence recovery, proportional to the concentration of the enzyme (in the range 0.4–7 nM), because of the separation of the dye from the quenching silica nanoparticle. The authors also proved the suitability of this system for multiplex imaging: they conjugated the same NP with three substrates specific for caspase-3, caspase-8 and caspase-9, each derivatized with a different dye, in such a way that each substrate would correspond to an emission in a different spectral region (490, 560 and 675 nm). After internalization of this nanosensor into HCT116 cells, fluorescence microscopy revealed very low intensities from all three channels, and a large increase of fluorescence was observed upon treatment of the same cells with TRAIL, an apoptosis-inducing ligand. As expected, low signals were observed when inhibitors for the three caspases were also added, demonstrating the possibility of designing nanostructured systems that can be used for imaging at the single cell level in the presence of multiple intracellular enzymes.

5 Conclusions

Luminescent silica nanoparticles play an important role in the development of nanomedicine because their intrinsic features well match most essential pre-requisites for their possible use in vivo. On the other hand, their brightness can reach intensities among the highest reported so far in the field of nanomaterials, allowing one to profit fully from the sensitivity and resolution offered by fluorescence spectroscopy. However, what really makes silica nanoparticles unique is, in our opinion, their versatility. For example, their ζ potential can be finely tuned to match the needs of a specific application (such as cell internalization or lymph node mapping), or their surface can be rather easily derivatized with suitable ligands to

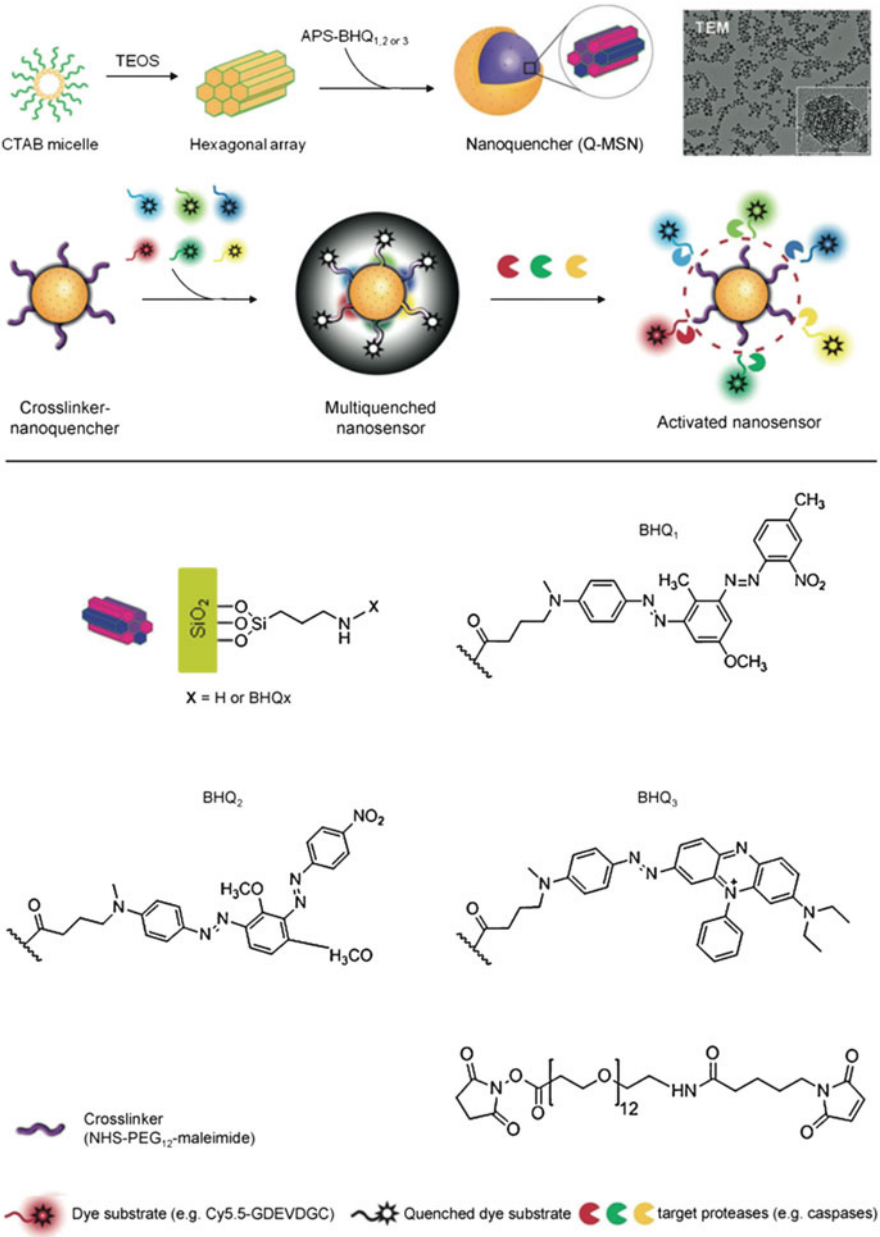

Fig. 10 Design of non-fluorescent and broad-spectrum nanoquencher and nanosensor. *Top*: diagram showing the synthesis of Q-MSNs. *Image*: TEM image of Q-MSNs. *Bottom*: chemical structures of the components of Q-MSNs (copyright Huang et al. [97])

obtain selective targeting. A highly synthetic versatility also offers the rare chance to design multichromophoric structures to obtain collective energy- and electron-transfer processes. These processes, as we have described in this review, are the basis of extremely valuable features. For example, with controlled, incomplete, energy transfer processes, nanoparticles presenting two or more emission signals can be advantageously used for barcoding applications or for carrying out in vivo and ex vivo experiments on the same subject using the same nanostructured probe. On the other hand, an almost complete energy transfer, when obtained with careful design, can be greatly beneficial, yielding a set of nanostructures which, excited at the same wavelength, can give bright luminescence of different colours, favouring multiplexing in microscopy and cytofluorimetry. These nanoparticles also present the additional advantages of minimizing self-quenching processes and increasing the separation between the excitation and the emission wavelengths, highly increasing the signal to noise ratio.

Finally, when designing nanoparticle-based chemosensors, collective energy- and electron-transfer processes can allow signal amplification, extending the possibility of monitoring important biological species and processes.

Notably, although many advantages are becoming evident, as we have discussed, additional potentials remain largely unexplored for these materials. We hope that the data discussed in this review article inspire a growing number of scientists to proceed in this direction, addressing more and more ambitious goals.

Acknowledgments We acknowledge financial support from the University of Bologna (FARB Project Advanced Ultrasensitive Multiplex Diagnostic Systems Based on Luminescence Techniques) and from Regione Lombardia-INSTM (Sinfonia project).

References

1. Hussain T, Nguyen QT (2014) Molecular imaging for cancer diagnosis and surgery. Adv Drug Deliv Rev 66:90–100
2. Tirotta I et al (2015) (19)F magnetic resonance imaging (MRI): from design of materials to clinical applications. Chem Rev 115(2):1106–1129
3. Abramczyk H, Brozek-Pluska B (2013) Raman imaging in biochemical and biomedical applications. Diagnosis and treatment of breast cancer. Chem Rev 113(8):5766–5781
4. Cutler CS et al (2013) Radiometals for combined imaging and therapy. Chem Rev 113 (2):858–883
5. Verwilst P et al (2015) Recent advances in Gd-chelate based bimodal optical/MRI contrast agents. Chem Soc Rev 44(7):1791–1806
6. Nie L, Chen X (2014) Structural and functional photoacoustic molecular tomography aided by emerging contrast agents. Chem Soc Rev 43(20):7132–7170
7. Zhu L, Ploessl K, Kung HF (2014) PET/SPECT imaging agents for neurodegenerative diseases. Chem Soc Rev 43(19):6683–6691
8. Montalti M et al (2014) Dye-doped silica nanoparticles as luminescent organized systems for nanomedicine. Chem Soc Rev, 43(12):4243–4268
9. Merian J et al (2012) Fluorescent nanoprobes dedicated to in vivo imaging: from preclinical validations to clinical translation. Molecules 17(5):5564–5591

10. Buckland J (2015) Experimental arthritis: in vivo noninvasive molecular optical imaging of disease. Nat Rev Rheumatol 11(5):258
11. Broome AM et al (2015) Optical imaging of targeted beta-galactosidase in brain tumors to detect EGFR levels. Bioconjug Chem 26(4):660–668
12. Anderson RR, Parrish JA (1981) The optics of human skin. J Invest Dermatol 77(1):13–19
13. Rocha U et al (2014) Neodymium-doped LaF(3) nanoparticles for fluorescence bioimaging in the second biological window. Small 10(6):1141–1154
14. Bi S et al (2015) A hot-spot-active magnetic graphene oxide substrate for microRNA detection based on cascaded chemiluminescence resonance energy transfer. Nanoscale 7(8):3745–3753
15. Nepomnyashchii AB, Bard AJ (2012) Electrochemistry and electrogenerated chemiluminescence of BODIPY dyes. Acc Chem Res 45(11):1844–1853
16. Wu P et al (2014) Electrochemically generated versus photoexcited luminescence from semiconductor nanomaterials: bridging the valley between two worlds. Chem Rev 114 (21):11027–11059
17. Di Fusco M et al (2015) Organically modified silica nanoparticles doped with new acridine-1,2-dioxetane analogues as thermochemiluminescence reagentless labels for ultrasensitive immunoassays. Anal Bioanal Chem 407(6):1567–1576
18. Gong H et al (2014) Engineering of multifunctional nano-micelles for combined photothermal and photodynamic therapy under the guidance of multimodal imaging. Adv Funct Mater 24 (41):6492–6502
19. Lv RC et al (2015) Multifunctional anticancer platform for multimodal imaging and visible light driven photodynamic/photothermal therapy. Chem Mater 27(5):1751–1763
20. Yi XM et al (2014) Near-infrared fluorescent probes in cancer imaging and therapy: an emerging field. Int J Nanomedicine 9:1347–1365
21. Wang R, Zhang F (2014) NIR luminescent nanomaterials for biomedical imaging. J Mater Chem B 2(17):2422–2443
22. Wu H et al (2014) Self-assembly-induced near-infrared fluorescent nanoprobes for effective tumor molecular imaging. J Mater Chem B 2(32):5302–5308
23. Li K, Liu B (2014) Polymer-encapsulated organic nanoparticles for fluorescence and photoacoustic imaging. Chem Soc Rev 43(18):6570–6597
24. Liberman A et al (2014) Synthesis and surface functionalization of silica nanoparticles for nanomedicine. Surf Sci Rep 69(2–3):132–158
25. Cassette E et al (2013) Design of new quantum dot materials for deep tissue infrared imaging. Adv Drug Deliv Rev 65(5):719–731
26. Jing LH et al (2014) Magnetically engineered semiconductor quantum dots as multimodal imaging probes. Adv Mater 26(37):6367–6386
27. Vivero-Escoto JL, Huxford-Phillips RC, Lin WB (2012) Silica-based nanoprobes for biomedical imaging and theranostic applications. Chem Soc Rev 41(7):2673–2685
28. Bonitatibus PJ et al (2012) Preclinical assessment of a Zwitterionic tantalum oxide nanoparticle X-ray contrast agent. ACS Nano 6(8):6650–6658
29. Caltagirone C et al (2014) Silica-based nanoparticles: a versatile tool for the development of efficient imaging agents. Chem Soc Rev 44(14):4645–4671
30. Toy R et al (2014) Targeted nanotechnology for cancer imaging. Adv Drug Deliv Rev 76:79–97
31. Li CH, Hu JM, Liu SY (2012) Engineering FRET processes within synthetic polymers, polymeric assemblies and nanoparticles via modulating spatial distribution of fluorescent donors and acceptors. Soft Matter 8(27):7096–7102
32. Ray PC et al (2014) Nanoscopic optical rulers beyond the FRET distance limit: fundamentals and applications. Chem Soc Rev 43(17):6370–6404
33. Genovese D et al (2014) Energy transfer processes in dye-doped nanostructures yield cooperative and versatile fluorescent probes. Nanoscale 6(6):3022–3036
34. Genovese D et al (2013) Prevention of self-quenching in fluorescent silica nanoparticles by efficient energy transfer. Angew Chem Int Ed 52(23):5965–5968

35. Biffi S et al (2014) Multiple dye-doped NIR-emitting silica nanoparticles for both flow cytometry and in vivo imaging. Rsc Adv 4(35):18278–18285
36. Meng HM et al (2015) Multiple functional nanoprobe for contrast-enhanced bimodal cellular imaging and targeted therapy. Anal Chem 87(8):4448–4454
37. Helle M et al (2013) Surface chemistry architecture of silica nanoparticles determine the efficiency of in vivo fluorescence lymph node mapping. ACS Nano 7(10):8645–8657
38. Jeon YH et al (2010) In vivo imaging of sentinel nodes using fluorescent silica nanoparticles in living mice. Mol Imaging Biol 12(2):155–162
39. Bonacchi S et al (2011) Luminescent silica nanoparticles: extending the frontiers of brightness. Angew Chem Int Ed 50(18):4056–4066
40. Montalti M et al (2013) Luminescent chemosensors based on silica nanoparticles for the detection of ionic species. New J Chem 37(1):28–34
41. Stöber W, Fink A, Bohn E (1968) Controlled growth of monodisperse silica spheres in the micron size range. J Colloid Interface Sci 26(1):62–69
42. Van Blaaderen A, Vrij A (1992) Synthesis and characterization of colloidal dispersions of fluorescent, monodisperse silica spheres. Langmuir 8(12):2921–2931
43. Wang J et al (2011) Two-phase synthesis of monodisperse silica nanospheres with amines or ammonia catalyst and their controlled self-assembly. ACS Appl Mater Interfaces 3(5):1538–1544
44. Larson DR et al (2008) Silica nanoparticle architecture determines radiative properties of encapsulated fluorophores. Chem Mater 20(8):2677–2684
45. Bagwe RP, Hilliard LR, Tan W (2006) Surface modification of silica nanoparticles to reduce aggregation and nonspecific binding. Langmuir 22(9):4357–4362
46. Zanarini S et al (2009) Iridium doped silica – PEG nanoparticles: enabling electrochemiluminescence of neutral complexes in aqueous media. J Am Chem Soc 131(40):14208–14209
47. Yong KT et al (2009) Multifunctional nanoparticles as biocompatible targeted probes for human cancer diagnosis and therapy. J Mater Chem 19(27):4655–4672
48. Bagwe RP et al (2004) Optimization of dye-doped silica nanoparticles prepared using a reverse microemulsion method. Langmuir 20(19):8336–8342
49. Kim S et al (2007) Organically modified silica nanoparticles co-encapsulating photosensitizing drug and aggregation-enhanced two-photon absorbing fluorescent dye aggregates for two-photon photodynamic therapy. J Am Chem Soc 129(9):2669–2675
50. Kim S et al (2007) Intraparticle energy transfer and fluorescence photoconversion in nanoparticles: an optical highlighter nanoprobe for two-photon bioimaging. Chem Mater 19(23):5650–5656
51. Selvestrel F et al (2013) Targeted delivery of photosensitizers: efficacy and selectivity issues revealed by multifunctional ORMOSIL nanovectors in cellular systems. Nanoscale 5(13):6106–6116
52. Kumar R et al (2008) Covalently dye-linked, surface-controlled, and bioconjugated organically modified silica nanoparticles as targeted probes for optical imaging. ACS Nano 2(3):449–456
53. Kumar R et al (2010) In vivo biodistribution and clearance studies using multimodal organically modified silica nanoparticles. ACS Nano 4(2):699–708
54. Seddon A, Li Ou D (1998) CdSe quantum dot doped amine-functionalized ormosils. J Solgel Sci Technol 13(1–3):623–628
55. Law W-C et al (2008) Optically and magnetically doped organically modified silica nanoparticles as efficient magnetically guided biomarkers for two-photon imaging of live cancer cells. J Phys Chem C 112(21):7972–7977
56. Ma K et al (2013) Controlling growth of ultrasmall sub-10 nm fluorescent mesoporous silica nanoparticles. Chem Mater 25(5):677–691
57. Rampazzo E et al (2010) Energy transfer from silica core – surfactant shell nanoparticles to hosted molecular fluorophores. J Phys Chem B 114(45):14605–14613

58. Chi F et al (2010) Size-tunable and functional core – shell structured silica nanoparticles for drug release. J Phys Chem C 114(6):2519–2523
59. Liu J et al (2009) Tunable assembly of organosilica hollow nanospheres. J Phys Chem C 114 (2):953–961
60. Rampazzo E et al (2012) Multicolor core/shell silica nanoparticles for in vivo and ex vivo imaging. Nanoscale 4(3):824–830
61. Cushing BL, Kolesnichenko VL, O'Connor CJ (2004) Recent advances in the liquid-phase syntheses of inorganic nanoparticles. Chem Rev 104(9):3893–3946
62. Gallagher D, Ring TA (1989) Chimia 43:298
63. Pedone A et al (2013) Understanding the photophysical properties of coumarin-based Pluronic-silica (PluS) nanoparticles by means of time-resolved emission spectroscopy and accurate TDDFT/stochastic calculations. Phys Chem Chem Phys 15(29):12360–12372
64. Valenti G et al (2012) A versatile strategy for tuning the color of electrochemiluminescence using silica nanoparticles. Chem Commun 48(35):4187–4189
65. Rampazzo E et al (2011) A versatile strategy for signal amplification based on core/shell silica nanoparticles. Chem Eur J 17(48):13429–13432
66. Genovese D et al (2011) Reversible photoswitching of dye-doped core-shell nanoparticles. Chem Commun 47(39):10975–10977
67. Soster M et al (2012) Targeted dual-color silica nanoparticles provide univocal identification of micrometastases in preclinical models of colorectal cancer. Int J Nanomedicine 7:4797–4807
68. Rampazzo E et al (2013) Proper design of silica nanoparticles combines high brightness, lack of cytotoxicity and efficient cell endocytosis. Nanoscale 5(17):7897–7905
69. Verhaegh NAM, Blaaderen AV (1994) Dispersions of rhodamine-labeled silica spheres: synthesis, characterization, and fluorescence confocal scanning laser microscopy. Langmuir 10(5):1427–1438
70. Smith JE et al (2007) Aptamer-conjugated nanoparticles for the collection and detection of multiple cancer cells. Anal Chem 79(8):3075–3082
71. Wang L et al (2007) Fluorescent nanoparticles for multiplexed bacteria monitoring. Bioconjug Chem 18(2):297–301
72. Wang L, Yang CY, Tan WH (2005) Dual-luminophore-doped silica nanoparticles for multiplexed signaling. Nano Lett 5(1):37–43
73. Chen XL et al (2009) Using aptamer-conjugated fluorescence resonance energy transfer nanoparticles for multiplexed cancer cell monitoring. Anal Chem 81(16):7009–7014
74. He XX et al (2012) Fluorescence resonance energy transfer mediated large Stokes shifting near-infrared fluorescent silica nanoparticles for in vivo small-animal imaging. Anal Chem 84 (21):9056–9064
75. Gutwein LG et al (2012) Fractionated photothermal antitumor therapy with multidye nanoparticles. Int J Nanomedicine 7:351–357
76. Prodi L (2005) Luminescent chemosensors: from molecules to nanoparticles. New J Chem 29 (1):20–31
77. Bonacchi S et al (2011) Luminescent chemosensors based on silica nanoparticles. Top Curr Chem 300:93–138
78. Lodeiro C et al (2010) Light and colour as analytical detection tools: a journey into the periodic table using polyamines to bio-inspired systems as chemosensors. Chem Soc Rev 39 (8):2948–2976
79. Montalti M et al (2014) Dye-doped silica nanoparticles as luminescent organized systems for nanomedicine. Chem Soc Rev 43(12):4243–4268
80. Que EL, Domaille DW, Chang CJ (2008) Metals in neurobiology: probing their chemistry and biology with molecular imaging (2008, 108:1517). Chem Rev 108(10):4328
81. Doussineau T et al (2010) On the design of fluorescent ratiometric nanosensors. Chem Eur J 16 (34):10290–10299

82. Bazzicalupi C et al (2013) Multimodal use of new coumarin-based fluorescent chemosensors: towards highly selective optical sensors for Hg2+ probing. Chem Eur J 19(43):14639–14653
83. Ambrosi G et al (2015) PluS nanoparticles as a tool to control the metal complex stoichiometry of a new thio-aza macrocyclic chemosensor for Ag(I) and Hg(II) in water. Sens Actuat B Chem 207:1035–1044
84. Arca M et al (2014) A fluorescent ratiometric nanosized system for the determination of Pd-II in water. Chem Commun 50(96):15259–15262
85. Qin Y et al (2013) Direct comparison of a genetically encoded sensor and small molecule indicator: implications for quantification of cytosolic Zn2+. ACS Chem Biol 8(11):2366–2371
86. Tsai Y-T et al (2014) Real-time noninvasive monitoring of in vivo inflammatory responses using a pH ratiometric fluorescence imaging probe. Adv Healthc Mater 3(2):221–229
87. Burns A et al (2006) Core/shell fluorescent silica nanoparticles for chemical sensing: towards single-particle laboratories. Small 2(6):723–726
88. Chen Y-P et al (2012) Surface charge effect in intracellular localization of mesoporous silica nanoparticles as probed by fluorescent ratiometric pH imaging. Rsc Adv 2(3):968–973
89. Doussineau T, Trupp S, Mohr GJ (2009) Ratiometric pH-nanosensors based on rhodamine-doped silica nanoparticles functionalized with a naphthalimide derivative. J Colloid Interface Sci 339(1):266–270
90. Peng J et al (2007) Noninvasive monitoring of intracellular pH change induced by drug stimulation using silica nanoparticle sensors. Anal Bioanal Chem 388(3):645–654
91. Wu S et al (2011) Dual colored mesoporous silica nanoparticles with pH activable rhodamine-lactam for ratiometric sensing of lysosomal acidity. Chem Commun 47(40):11276–11278
92. Meng Q et al (2010) Multifunctional mesoporous silica material used for detection and adsorption of Cu2+ in aqueous solution and biological applications in vitro and in vivo. Adv Funct Mater 20(12):1903–1909
93. Seo S et al (2010) Fluorescein-functionalized silica nanoparticles as a selective fluorogenic chemosensor for Cu2+ in living cells. Eur J Inorg Chem 2010(6):843–847
94. Zeng L et al (2005) A selective turn-on fluorescent sensor for imaging copper in living cells. J Am Chem Soc 128(1):10–11
95. Bau L, Tecilla P, Mancin F (2011) Sensing with fluorescent nanoparticles. Nanoscale 3(1):121–133
96. Bae SW et al (2010) Apoptotic cell imaging using phosphatidylserine-specific receptor-conjugated Ru(bpy)32 + -doped silica nanoparticles. Small 6(14):1499–1503
97. Huang X et al (2012) Multiplex imaging of an intracellular proteolytic cascade by using a broad-spectrum nanoquencher. Angew Chem Int Ed 51(7):1625–1630